

Control of the inhomogeneity degree by magnetic dilution in crystals of antiferromagnetic molecular rings

J. J. Henderson, C. M. Ramsey, and E. del Barco*

Department of Physics, University of Central Florida, Orlando, Florida 32816, USA

T. C. Stamatatos and G. Christou

Department of Chemistry, University of Florida, Gainesville, Florida 32611, USA

(Received 12 November 2008; published 9 December 2008)

Employing the electron spin in solid-state qubits is considered a promising method for quantum information processing. In this context, we present a microwave spectroscopic study on magnetically dilute crystals of Fe_{18} antiferromagnetic molecular rings. Doping with Ga^{3+} , at concentrations ranging from 0.5% down to 0.005%, results in magnetic Fe_{17}Ga ($S=5/2$) molecules dispersed throughout the lattice, with 2–8 nm average intermolecular separation. The results reveal a significant decrease in the degree of inhomogeneity of the system, hinting at a controlled reduction in decoherence mechanisms inherent to an ensemble of anisotropic molecular magnets while maintaining the crystalline order.

DOI: 10.1103/PhysRevB.78.214413

PACS number(s): 75.50.Tt, 75.45.+j, 75.60.Lr

Significant efforts have been devoted to the study of the quantum dynamics of molecular magnets in view of their possible use in quantum information technologies^{1–11} and as a means of enhancing the knowledge of the poorly understood process of decoherence in nanoscale systems.^{12–16} Along these lines, it seems that intermolecular dipolar interactions, which considerably shorten the coherence times in concentrated samples, have stymied progress in this direction. Proposals to overcome this limitation include antiferromagnetic (AFM) molecular wheels, which have received considerable attention during the last years,^{17–33} mostly due to potentially longer coherence times associated to the dynamics of the Néel vector.^{15,16}

Recent experimental works^{31–34} have established that, in order to study intrinsic decoherence mechanisms of the electron spin in molecular nanomagnets, dephasing caused by fluctuating dipolar interactions needs to be eliminated. One approach, followed by Ardavan *et al.*,³¹ Bertaina *et al.*,³² and Schlegel *et al.*,³³ consists in diluting the molecular nanomagnets in solution until obtaining a significant intermolecular separation. In these studies the authors found that the transverse relaxation times in molecular magnets are ultimately limited by nuclear hyperfine interactions while still showing remarkably long dephasing times ($\tau_\phi < 3 \mu\text{s}$). Unfortunately, the dilution of molecular magnets in solution conveys a dispersion of the molecular spin orientation and anisotropy axes (among other effects), significantly influencing the energy landscape of the magnetic levels and causing the molecules within the sample to respond differently upon application of an external perturbation, such as a magnetic-field or electromagnetic irradiation. Following an alternative approach, recently reported by Takahashi *et al.*,³⁴ a large magnetic field was used to polarize the spin bath in a condensed crystalline sample of Fe_8 single-molecule magnets (SMMs), a method that was previously shown to work successfully to eliminate the dipolar dephasing mechanism in nitrogen impurities in diamond.³⁵ However, the spin-bath polarization requirement substantially restricts the experimental conditions of the experiment to low temperatures, large magnetic

fields, and high frequencies, which imposes limitations for the phenomenology under study. This is particularly important in molecular nanomagnets, in which large magnetic fields wipe out the anisotropy intrinsic to the system.

In this paper we present a detailed electron paramagnetic resonance (EPR) study of single crystals of AFM Fe_{18} wheels in which, as a result of controlled doping with Ga, only a small percentage of the molecules possesses a magnetic ground state, in effect minimizing intermolecular dipolar interactions while still preserving the monodispersity of a crystalline system. The latter is evidenced by the cleanness of the EPR spectra, showing absorption peaks associated to transitions between the spin levels of the resultant magnetic Fe_{17}Ga wheels that narrow as the dilution level (i.e., intermolecular distance) increases.

Specifically, we studied single crystals of a new family of $[\text{Fe}_{18}(\text{pd})_{12}(\text{pdH})_{12}(\text{O}_2\text{CR}_6)(\text{NO}_3)_6](\text{NO}_3)_6$ ferric wheels, constituting antiferromagnetic rings of 18 Fe^{3+} ions.¹⁹ This Fe_{18} compound crystallizes as large cubic crystals in rhombohedral space group $R\bar{3}$ and in high overall yields $>85\%$. The Fe^{3+} ($S=5/2$) ions were controllably substituted with Ga^{3+} ($S=0$) to produce antiferromagnetic Fe_{17}Ga wheels with a ground-state spin value of $5/2$. The molecular structure and spin configuration of a wheel singly doped with a Ga^{3+} ion is shown in Fig. 1(a). The Ga^{3+} concentration was varied during the synthesis to statistically produce well-dispersed $S=5/2$ wheels diluted within a sea of antiferromagnetic isostructural molecules [see Fig. 1(b)]. Note that magnetic dopants have been previously used as spin markers to help determine the intrinsic magnetic anisotropy and intramolecular exchange coupling constants in single crystals of antiferromagnetic molecular wheels (i.e., Abbati *et al.*³⁶ made use of Fe doping at a 10% concentration to characterize Ga_6 wheels). However, to the best of our knowledge, there is no previous study on the effect of magnetic dilution on the dynamics of crystalline samples of molecular nanomagnets. In the present case, Ga:Fe doping concentrations ranging from 0.5% down to 0.005% result in average distances between magnetic molecules varying from 2 up to 8

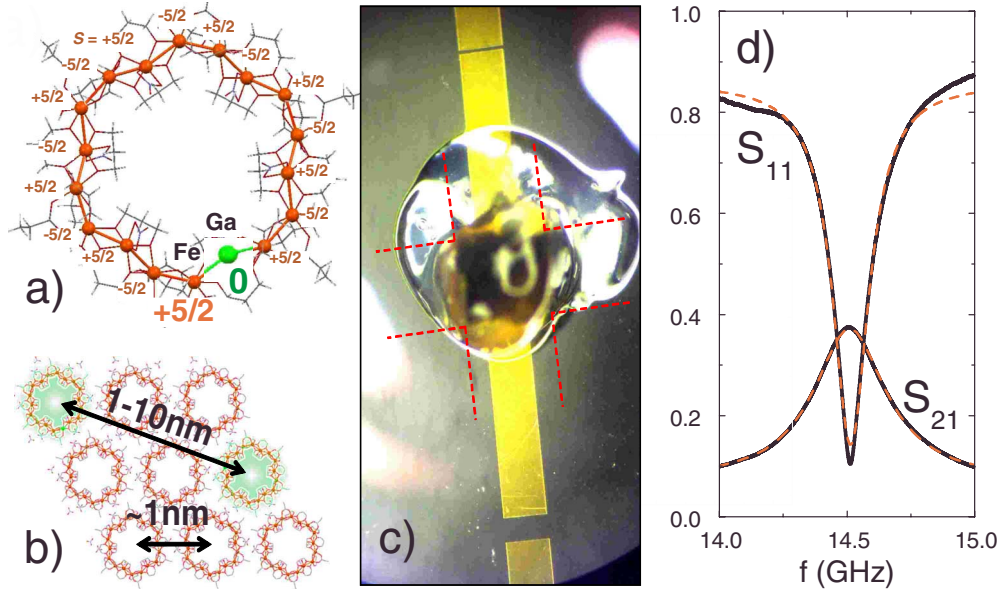


FIG. 1. (Color online) (a) Molecular structure of a Fe_{18} (Fe^{3+} , $S=5/2$) antiferromagnetic wheel doped with a single Ga^{3+} ($S=0$). This doping leads to spin noncompensation and a magnetic ground state $S=5/2$ at low temperature. (b) Representation of the magnetic dilution achieved in a single crystal of Fe_{18} molecular wheels by controlling the average separation between magnetic molecules through Ga doping. (c) Optical micrograph of a microstrip resonator. A typical $\text{Fe}_{18}:\text{Ga}$ crystal can be seen mounted on the 0.4-mm-wide microstrip line resonator with vacuum grease. (d) Room-temperature transmission (S_{21}) and reflection (S_{11}) parameters of the microstrip line resonator used in the experiments.

nm. Elemental analysis carried out on the studied samples (not shown) confirms the mentioned doping ratio for concentrations over 0.1%, below which the technique is not sensitive enough. The significance of this control lies in the ability to diminish the dephasing due to dipolar interactions between the magnetic molecules, which is inversely proportional to the cube of the intermolecular distance ($\tau_d \sim f_0 S^2 / d^3$ with $f_0 \sim 100$ MHz). In our case, dipolar dephasing times up to $\sim 1 \mu\text{s}$ are expected for the lowest concentration ($c=0.005\%$).

Low-frequency EPR measurements were obtained using a high sensitivity microstrip line resonator fabricated via optical lithography on a GaAs wafer.³⁷ An optical micrograph of a resonator designed to work with its fundamental mode at 9.7 GHz is shown in Fig. 1(c). Figure 1(d) shows the room-temperature transmission (S_{21}) and reflection (S_{11}) parameters of the microstrip line resonator used in the experiments. Although with moderately low quality factors ($Q \sim 100$), a large filling factor makes these resonators of extremely high sensitivity and entirely adequate for the investigation of highly dilute submillimeter crystals of molecular magnets. A typical $\text{Fe}_{18}:\text{Ga}$ single crystal can be seen mounted on a 400- μm -wide resonator with vacuum grease. Preliminary angular dependence EPR measurements performed on these crystals (not shown) reveal a magnetic axial symmetry along the principal rotational axis of the molecular wheels. The EPR spectra ($f=9.7$ GHz) of a Fe_{18} single crystal doped at a 0.005% Ga:Fe concentration measured at different temperatures ($T=0.3, 1.8,$ and 4.5 K) with the magnetic field oriented along the wheel axis (axial anisotropy axis) are presented in Fig. 2. Data in Fig. 2 have been averaged over 30 field sweeps due to the weak signal obtained for such a low-concentration crystal. Four peaks are clearly visible in the

spectra. Three peaks, with their indices denoting $|S_z|$, originate from transitions between levels with the same $|S_z|$ value, where $S_z = -S, \dots, +S$ are the projections of the spin, S , of the Fe_{17}Ga molecules onto the z axis (i.e., wheel axis). The peaks labeled as “ $(-1/2, 3/2)$ ” and “ α ” correspond to transitions between states of different spin projections (from spin

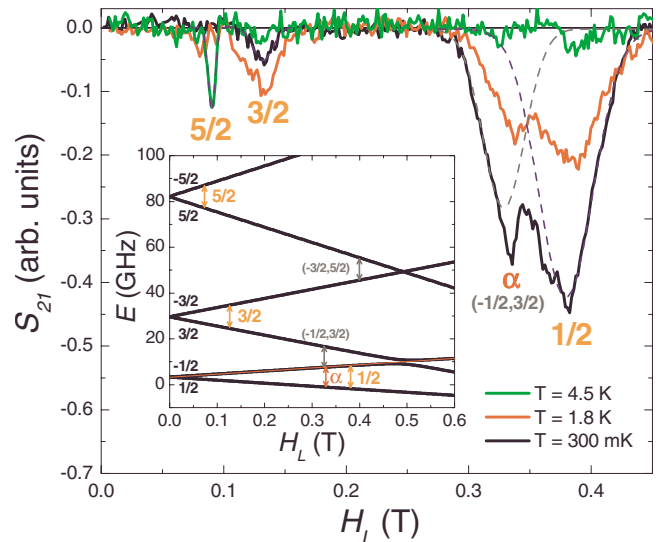


FIG. 2. (Color online) EPR spectra of 9.7 GHz as a function of the longitudinal magnetic field, H_L , recorded at different temperatures on a single crystal of Fe_{18} molecular wheels doped with Ga at a concentration of 0.005% (Ga:Fe). Inset: energy level diagram calculated by direct diagonalization of the Hamiltonian given in Eq. (1) (see text for parameter values) with the magnetic field aligned along the wheel z axis. All indicated transitions correspond to the peaks observed in the main figure.

level $S_z = -1/2$ to $S_z = +3/2$ in this particular case). In addition, a weak contribution from a Fe mononuclear impurity ($g=2$), which we attribute to be located at the crystal surface and is also found in pure Fe_{18} antiferromagnetic crystals (not shown), is expected at this field value.

The behavior of the EPR peaks with temperature indicates that the $|S_z|=1/2$ spin projections are the molecule ground states, which determines a positive axial anisotropy parameter ($D>0$) in the spin Hamiltonian. Gaussian functions have been used to fit the peaks (dashed lines in Fig. 2); at the lowest temperature they become visible. The largest peak at low temperature corresponds to the $-1/2 \rightarrow +1/2$ transition and has a linewidth of ~ 440 G. The $-3/2 \rightarrow +3/2$ and $-5/2 \rightarrow +5/2$ transition peaks have linewidths of ~ 160 and ~ 40 G, respectively. The fact that the peak widths do not follow the 5:3:1 ratio associated to the spin levels involved in each transition can be understood in terms of a transverse anisotropy term which affects (curves) the Zeeman energy of the levels. In addition, the shift of the “1/2” peak from 0.33 T, expected from a linear Zeeman splitting between opposite spin-1/2 projections, to 0.38 T is also indicative of a symmetry-lowering perturbation curving the field behavior of the levels. We attribute this to the substituting Ga ion, which certainly breaks the high symmetry of the AFM wheel, most likely generating a twofold symmetry axis within the plane of each molecule, as discussed below.

The small linewidths (>40 G) of these transitions illuminate one advantage of the single-crystal dilution method. In the case of the dilute solution sample of Cr_7Mn rings with anisotropy studied by Ardavan,³¹ the overall linewidth was 5000 G due to orientational averaging in the frozen glass sample, complicating the elucidation of the transitions excited at a given field. Similarly, linewidths over 500 G were found by Bertaina *et al.*³² in samples of isotropic magnetic molecules, where the degree of inhomogeneity of the system is intrinsically lower. In contrast, through a determination of the spin-Hamiltonian parameters, it is possible to know the spin energy landscape for a single crystal oriented in any magnetic-field direction.

EPR spectra as a function of a transverse magnetic field (applied perpendicularly to the wheels axes) that have also been recorded on the same crystal are shown in Fig. 3. Two peaks are clearly observed at and for the same frequency and temperatures than the data presented in Fig. 2. The results are shown in Fig. 3. The peaks are found at ~ 0.14 T ($\Delta_{1/2}$) and ~ 0.37 T ($\Delta_{3/2}$). These peaks are generated by transitions between superposition states of opposite spin projections and split by an energy Δ_{ij} ($i=-j$, with $i=1/2$ and $3/2$, respectively) by the action of the transverse field. Note that the external magnetic field produces a mixture of spin levels, making the states associated to the EPR transitions to be linear combinations of all the S_z projections rather than a clean superposition of only two opposite spin projections. The nomenclature followed here is just intended to abbreviate the discussion. The weak contribution of the paramagnetic impurity is observed as a small peak (α) at ~ 0.33 T. The overall decrease in the magnitude of the peaks at higher temperatures, also observed in longitudinal field EPR spectra recorded up to 15 K (not shown), suggests the presence of excited states. This is confirmed by high-frequency EPR

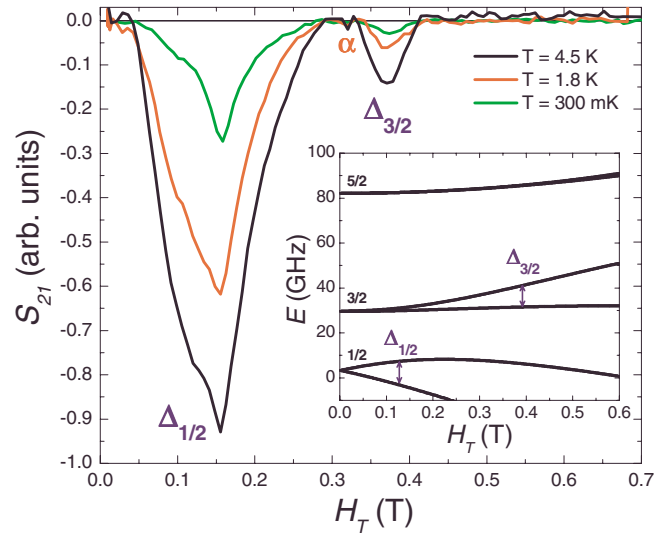


FIG. 3. (Color online) EPR spectra of 9.7 GHz as a function of the transverse magnetic field, H_T , recorded at different temperatures on a single crystal of Fe_{18} molecular wheels doped with Ga at a concentration of 0.005% (Ga:Fe). Inset: energy level diagram calculated by direct diagonalization of the Hamiltonian given in Eq. (1) (see text) with the magnetic field perpendicular to the z axis of the wheel. The blue arrows indicate the transitions corresponding to the peaks observed in the main figure.

experiments carried out by Stephen Hill³⁸ in both doped and undoped crystals of Fe_{18} wheels, where higher frequency (>50 GHz) absorption peaks are associated to excited states ($S>0$) of the undoped AFM molecules. However, at the low magnetic fields and frequency used in our experiments, excited states do not play any relevant role on the observations.

We associate the larger widths of the transverse field EPR transitions (in comparison to the longitudinal field spectra) to the introduction of a single Ga^{3+} ion, which, as said above, imposes a twofold symmetry on the ring, generating a second-order transverse anisotropy term in the Hamiltonian. Because we sample an ensemble of molecules in the crystal rather than one molecule at a time, based on statistics, EPR spectra are not expected to reveal the twofold symmetry associated to each individual molecule since different molecules throughout the crystal present different orientations of the transverse anisotropy axes, which are determined by the arbitrary position of the Ga ion in each of the wheels. Consequently, broader transverse field EPR peaks are anticipated as a result of the angular dispersion of the transverse anisotropy axes within the crystal. Figure 4 shows the positions of the absorption peaks, $\Delta_{1/2}$ and $\Delta_{3/2}$, extracted from EPR measurements for different orientations, ϕ , of a transverse field applied in the plane of the molecular wheels for the same 0.005% Ga:Fe diluted crystal. The absence of modulation (within the noise of the measurement) confirms the dispersion of the molecular transverse anisotropy axes within the crystal.

The spin Hamiltonian which best describes the Fe_{17}Ga molecular magnet is

$$H = DS_z^2 + E(S_x^2 - S_y^2) - \mu_B \mathbf{S} \cdot \hat{g} \cdot \mathbf{H}, \quad (1)$$

where the first two terms correspond to the uniaxial and transverse anisotropies of the molecule and the last term is

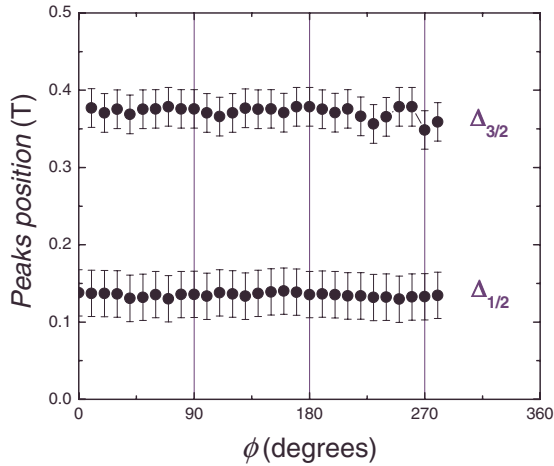


FIG. 4. (Color online) Position of the 9.7 GHz EPR absorption peaks as a function of the angle of application of the transverse field within the plane of the wheel. The experiments have been performed at $T=300$ mK on a single crystal of Fe_{18} molecular wheels doped with Ga at a concentration of 0.005% (Ga:Fe).

the Zeeman energy associated to the coupling between the molecule spin and the external field. The values $D=+0.63$ K, $E=10$ mK, $g_z=1.9$, and $g_{\perp}=2.3$ are found to best explain the experimental results. Note that a positive value of D imposes an easy magnetic plane parallel to the wheel plane. The given values of the Hamiltonian parameters, particularly in the case of the transverse terms, E and g_{\perp} (the value of the latter is unusually large) need to be taken just as rough estimates due to the uncertainty in the position of the Ga ions for different wheels. Of special relevance is the fact that the spin-Hamiltonian parameters allow us to construct the spin energy levels diagram for any magnetic-field orientation, as displayed in the insets of Figs. 2 and 3 with the field applied both longitudinal and transverse to the wheel z axis, respectively. The arrows highlight the resonances observed in the respective main figures. The symmetry-lowering effect imposed by the Fe-Ga substitution can be easily seen as a curvature of the levels due to degeneracy breaking at the anticrossing between levels of opposite spin projections (see level repulsion at ~ 0.48 T in the inset of Fig. 2). The second-order anisotropy parameter, E , was not included in the calculation ($E=0$) of the energy levels as a function of the transverse field since different molecules will present different relative orientations between the applied field and their transverse anisotropy axes depending on the position of the Ga ion within the wheel. Therefore, the levels in the inset of Fig. 3 correspond to the average expected behavior of the whole crystal.

In order to understand the effect of the magnetic dilution of our crystals we have averaged the EPR spectra over 50 measurements recorded at 5 K while sweeping the longitudinal field through the peak associated to transitions between the $|S_z|=5/2$ spin projections. Note that this is the peak whose width is least affected by the transverse anisotropy (far from the anticrossing points). The resulting EPR absorption peaks (with normalized area) corresponding to the studied Ga:Fe concentrations are shown in Fig. 5(a). The peak narrows and slightly moves to low fields for decreasing con-

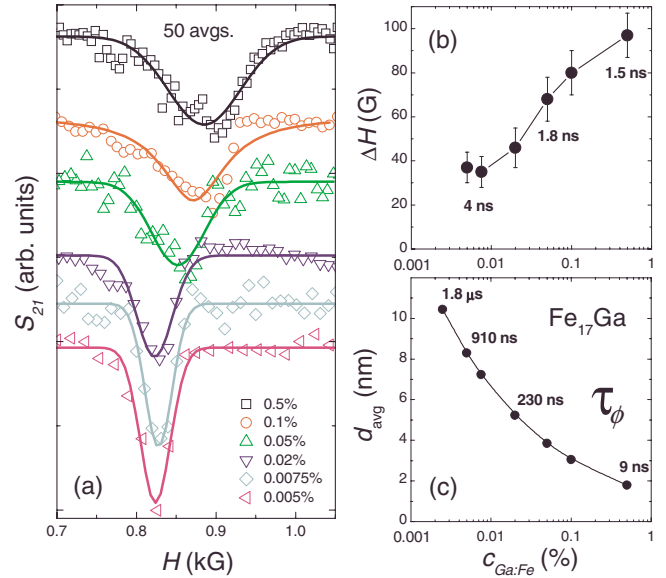


FIG. 5. (Color online) (a) Behavior of the EPR peak corresponding to the $S_z = \pm 5/2$ transition at 9.7 GHz as a function of the Ga:Fe doping concentration (0.005%–0.5%). (b) Peak's width versus concentration. The dephasing times extracted from the peak's width are shown below some of the data. (c) Calculated average distance between magnetic molecules (Fe_{17}Ga) as a function of the concentration. The calculated dipolar dephasing time associated to the average intermolecular distance is provided for some of the data.

centrations until saturating below $c \sim 0.01\%$. This can be clearly seen in Fig. 5(b), where the width of the peak is plotted as a function of the concentration. The times next to the data in Fig. 5(b) are estimates of the dephasing times extracted from the peak widths (varying from 1.5 to 4 ns), which are to be taken just as lower bounds due to the presence of inhomogeneous broadening. In Fig. 5(c), it is shown the average distance between magnetic molecules within the crystal as a function of doping concentration. The times given next to the data are the dipolar dephasing times calculated from the average distance (varying from 9 ns to 1.8 μs). The latter are overestimates since, in a crystal, molecules closer to each other than the average distance used in the calculation will contribute to the broadening of the peak, which explains the difference between the given dephasing times for the highest-concentration sample. The overall disparity between the estimated and calculated relaxation times evidences the inhomogeneous nature of the peak broadening, which is mostly due to dipolar interactions for high-concentration samples.³⁹ In addition, the saturation of the peak's width and position for low concentrations indicates an intrinsic dispersion of the structural or magnetic parameters of the crystal. Note that dipolar interactions are expected not only to broaden the peaks but also to change the average position of the EPR peaks when combined with other dispersion mechanisms intrinsic to the system, such as distribution of anisotropy parameters or anisotropy axes orientations. In our case, where different molecules present different orientations of the transverse anisotropy axes, the reduction in the dipolar fields conveys a reduction in the transverse fields felt

by the molecules and, consequently, the curvature of the levels weakens at low doping concentrations (level repulsion increases with transverse field), shifting the resonance condition to lower fields, as observed in the data.

Our results exemplify how the magnetic dilution of single crystals decreases the degree of inhomogeneity of the system while preserving the crystalline monodispersity. This method allows the study of the quantum dynamics of molecular magnets in solid-state form without the restrictions imposed by

the spin-bath polarization approach.^{34,35} Further experiments in this direction using pulsed-EPR measurements on crystals with low doping concentrations are the focus of our immediate plans.

We acknowledge fruitful discussions with Stephen Hill and Saiti Datta. We acknowledge support from the U.S. National Science Foundation under Grants No. DMR0737802 and No. DMR0747587 (J.J.H. and E.d.B.) and Grants No. DMR-0506946 and No. CHE-0414555 (G.C. and T.C.S.).

*delbarco@physics.ucf.edu

- ¹M. Leuenberger and D. Loss, *Nature (London)* **410**, 789 (2001).
- ²F. Meier, J. Levy, and D. Loss, *Phys. Rev. Lett.* **90**, 047901 (2003).
- ³M. Affronte, F. Troiani, A. Ghirri, A. Candini, M. Evangelisti, V. Corradini, S. Carretta, P. Santini, G. Amoretti, F. Tuna, G. Timco, and R. E. P. Winpenny, *J. Phys. D* **40**, 2999 (2007).
- ⁴D. Gatteschi, A. Caneschi, L. Pardi, and R. Sessoli, *Science* **265**, 1054 (1994).
- ⁵J. R. Friedman, M. P. Sarachik, J. Tejada, and R. Ziolo, *Phys. Rev. Lett.* **76**, 3830 (1996).
- ⁶L. Thomas, F. Lioni, R. Ballou, D. Gatteschi, R. Sessoli, and B. Barbara, *Nature (London)* **383**, 145 (1996).
- ⁷S. Hill, R. S. Edwards, N. Aliaga-Alcalde, and G. Christou, *Science* **302**, 1015 (2003).
- ⁸R. Amigó, J. M. Hernandez, A. García-Santiago, and J. Tejada, *Appl. Phys. Lett.* **82**, 4528 (2003).
- ⁹E. del Barco, A. D. Kent, E. C. Yang, and D. N. Hendrickson, *Phys. Rev. Lett.* **93**, 157202 (2004).
- ¹⁰M. Bal, J. R. Friedman, Y. Suzuki, E. M. Rumberger, D. N. Hendrickson, N. Avraham, Y. Myasoedov, H. Shtrikman, and E. Zeldov, *Europhys. Lett.* **71**, 110 (2005).
- ¹¹C. M. Ramsey, E. del Barco, S. Hill, S. J. Shah, C. C. Beedle, and D. N. Hendrickson, *Nat. Phys.* **4**, 277 (2008).
- ¹²N. V. Prokof'ev and P. C. E. Stamp, *Phys. Rev. Lett.* **80**, 5794 (1998).
- ¹³P. C. E. Stamp and I. S. Tupitsyn, *Phys. Rev. B* **69**, 014401 (2004).
- ¹⁴E. M. Chudnovsky, *Phys. Rev. Lett.* **92**, 120405 (2004).
- ¹⁵A. Chiolero and D. Loss, *Phys. Rev. Lett.* **80**, 169 (1998).
- ¹⁶F. Meier and D. Loss, *Phys. Rev. Lett.* **86**, 5373 (2001).
- ¹⁷C. Cañada-Vilalta, T. A. O'Brien, M. Pink, E. R. Davidson, and G. Christou, *Inorg. Chem.* **42**, 7819 (2003).
- ¹⁸C. Cañada-Vilalta, M. Pink, and G. Christou, *Chem. Commun. (Cambridge)* **2003**, 1240.
- ¹⁹P. King, T. C. Stamatatos, K. A. Abboud, and G. Christou, *Angew. Chem., Int. Ed.* **45**, 7379 (2006).
- ²⁰R. Bagai, K. A. Abboud, and G. Christou, *Chem. Commun. (Cambridge)* **2007**, 3359.
- ²¹T. C. Stamatatos, A. G. Christou, C. M. Jones, B. J. O'Callaghan, K. A. Abboud, T. A. O'Brien, and G. Christou, *J. Am. Chem. Soc.* **129**, 9840 (2007).
- ²²I. M. Atkinson, C. Benelli, M. Murrie, S. Parsons, and R. E. P. Winpenny, *Chem. Commun. (Cambridge)* **1999**, 285.
- ²³J. van Slageren, R. Sessoli, D. Gatteschi, A. A. Smith, M. Hellwell, R. E. P. Winpenny, A. Cornia, A.-L. Barra, A. G. M. Jansen, E. Rentschler, and G. A. Timco, *Chem. - Eur. J.* **8**, 277 (2002).
- ²⁴A. Cornia, M. Affronte, A. G. M. Jansen, G. L. Abbati, and D. Gatteschi, *Angew. Chem., Int. Ed.* **38**, 2264 (1999).
- ²⁵M. Affronte, T. Guidi, R. Caciuffo, S. Carretta, G. Amoretti, J. Hinderer, I. Sheikin, A. G. M. Jansen, A. A. Smith, R. E. P. Winpenny, J. van Slageren, and D. Gatteschi, *Phys. Rev. B* **68**, 104403 (2003).
- ²⁶O. Waldmann, T. Guidi, S. Carretta, C. Mondelli, and A. L. Dearden, *Phys. Rev. Lett.* **91**, 237202 (2003).
- ²⁷O. Waldmann, C. Dobe, H. Mutka, A. Furrer, and H. U. Güdel, *Phys. Rev. Lett.* **95**, 057202 (2005).
- ²⁸O. Waldmann, *Coord. Chem. Rev.* **249**, 2550 (2005).
- ²⁹L. Schnelzer, O. Waldmann, M. Horvatić, S. T. Ochsenbein, S. Krämer, C. Berthier, H. U. Güdel, and B. Pilawa, *Phys. Rev. Lett.* **99**, 087201 (2007).
- ³⁰J. Schnack and M. Luban, *Phys. Rev. B* **63**, 014418 (2000).
- ³¹A. Ardavan, O. Rival, J. J. L. Morton, S. J. Blundell, A. M. Tyryshkin, G. A. Timco, and R. E. P. Winpenny, *Phys. Rev. Lett.* **98**, 057201 (2007).
- ³²S. Bertaina, S. Gambarelli, T. Mitra, B. Tsukerblat, A. Müller, and B. Barbara, *Nature (London)* **453**, 203 (2008).
- ³³C. Schlegel, J. van Slageren, M. Manoli, E. K. Brechin, and M. Dressel, *Phys. Rev. Lett.* **101**, 147203 (2008).
- ³⁴S. Takahashi, J. van Tol, C. C. Beedle, D. N. Hendrickson, L.-C. Brunel, and M. S. Sherwin, arXiv:0810.1254 (unpublished).
- ³⁵S. Takahashi, R. Hanson, J. van Tol, M. S. Sherwin, and D. D. Awschalom, *Phys. Rev. Lett.* **101**, 047601 (2008).
- ³⁶G. L. Abbati, L.-C. Brunel, H. Casalta, A. Cornia, A. C. Fabretti, D. Gatteschi, A. K. Hassan, A. G. M. Jansen, A. L. Maniero, L. Pardi, C. Paulsen, and U. Segre, *Chem. - Eur. J.* **7**, 1796 (2001).
- ³⁷H. M. Quddusi, C. M. Ramsey, J. C. Gonzalez-Pons, J. J. Henderson, E. del Barco, G. de Loubens, and A. D. Kent, *Rev. Sci. Instrum.* **79**, 074703 (2008).
- ³⁸Stephen Hill (private communication).
- ³⁹Synthesis with Ga:Fe concentrations larger than 0.5% did not lead to stable crystals to be measured.